JEM Article

Enterocyte-specific A20 deficiency sensitizes to tumor necrosis factor-induced toxicity and experimental colitis

Lars Vereecke,^{1,2} Mozes Sze,^{1,2} Conor Mc Guire,^{1,2} Brecht Rogiers,^{1,2} Yuanyuan Chu,³ Marc Schmidt-Supprian,³ Manolis Pasparakis,⁴ Rudi Beyaert,^{1,2} and Geert van Loo^{1,2}

A20 is a nuclear factor κB (NF-κB) target gene that encodes a ubiquitin-editing enzyme that is essential for the termination of NF-κB activation after tumor necrosis factor (TNF) or microbial product stimulation and for the prevention of TNF-induced apoptosis. Mice lacking A20 succumb to inflammation in several organs, including the intestine, and A20 mutations have been associated with Crohn's disease. However, ablation of NF-κB activity, specifically in intestinal epithelial cells (IECs), promotes intestinal inflammation. As A20 deficiency sensitizes cells to TNF-induced apoptosis yet also promotes NF-κB activity, it is not clear if A20 deficiency in IECs would exacerbate or ameliorate intestinal inflammation. We generated mice lacking A20 specifically in IECs. These mice did not show spontaneous intestinal inflammation but exhibited increased susceptibility to experimental colitis, and their IECs were hypersensitive to TNF-induced apoptosis. The resulting TNF-driven breakdown of the intestinal barrier permitted commensal bacterial infiltration and led to systemic inflammation. These studies define A20 as a major antiapoptotic protein in the intestinal epithelium and further indicate that defects in A20 might contribute to inflammatory bowel disease in humans.

CORRESPONDENCE
Geert van Loo:
geert.vanloo@dmbr.vib-UGent.be
OR
Rudi Beyaert:
rudi.beyaert@dmbr.vib-UGent.be

Abbreviations used: A20IEC-KO, IEC-specific A20 knockout; CD, Crohn's disease; DSS, dextran sodium sulphate; ES, embryonic stem; IBD, inflammatory bowel disease; IEC, intestinal epithelial cell; IKK, IKB kinase; MEF, mouse embryonic fibroblast; NEMO, NF-KB essential modulator; NLR, NOD-like receptor; TLR, toll-like receptor; TNFR, TNF receptor.

Inflammatory bowel disease (IBD) and, in particular, Crohn's disease (CD), is thought to result from a dysregulated interaction between the host immune system and normal luminal microflora (Rakoff-Nahoum et al., 2006; Artis, 2008; Round and Mazmanian, 2009). Furthermore, epidemiological and linkage studies suggest a genetic predisposition and the involvement of environmental factors (Podolsky, 2002). The aberrant immune response in IBD is most likely facilitated by defects in both the barrier function of the intestinal epithelium and the mucosal immune system. Recognition of commensal bacterial products by toll-like receptors (TLRs) and NODlike receptors (NLRs) leads to the production of a mix of inflammatory cytokines and chemokines by immune cells and surface epithelial cells (Rakoff-Nahoum et al., 2004; Baumgart and Carding, 2007). In this context, the transcription factor NF-kB, which is activated by TLRs, NLRs, and cytokine receptors, such as TNF and

R. Beyaert and G. van Loo contributed equally to this paper.

IL-1, plays a critical role. On the one hand, NFκB regulates the expression of various cytokines and other modulators of the inflammatory processes in IBD. On the other hand, NF-kB enhances the survival of cells through the regulation of antiapoptotic genes. A tight regulation of the NF-kB signaling pathway and the genes induced is thus an absolute requirement. Recently, significant progress has been made in our understanding of the mechanisms that control the dynamics of NF-κB activation, and several autoregulatory feedback loops terminating the NF-kB response have been described (Renner and Schmitz, 2009). In this context, the NF-κB-responsive and ubiquitin-editing protein A20 (also referred to as TNF- α -induced protein 3 or TNFAIP3) has been described as a central gatekeeper in inflammation and immunity (Coornaert et al., 2009).

Downloaded from http://rupress.org/jem/article-pdf/207/7/1513/1903650/jem_20092474.pdf by guest on 02 December 2025

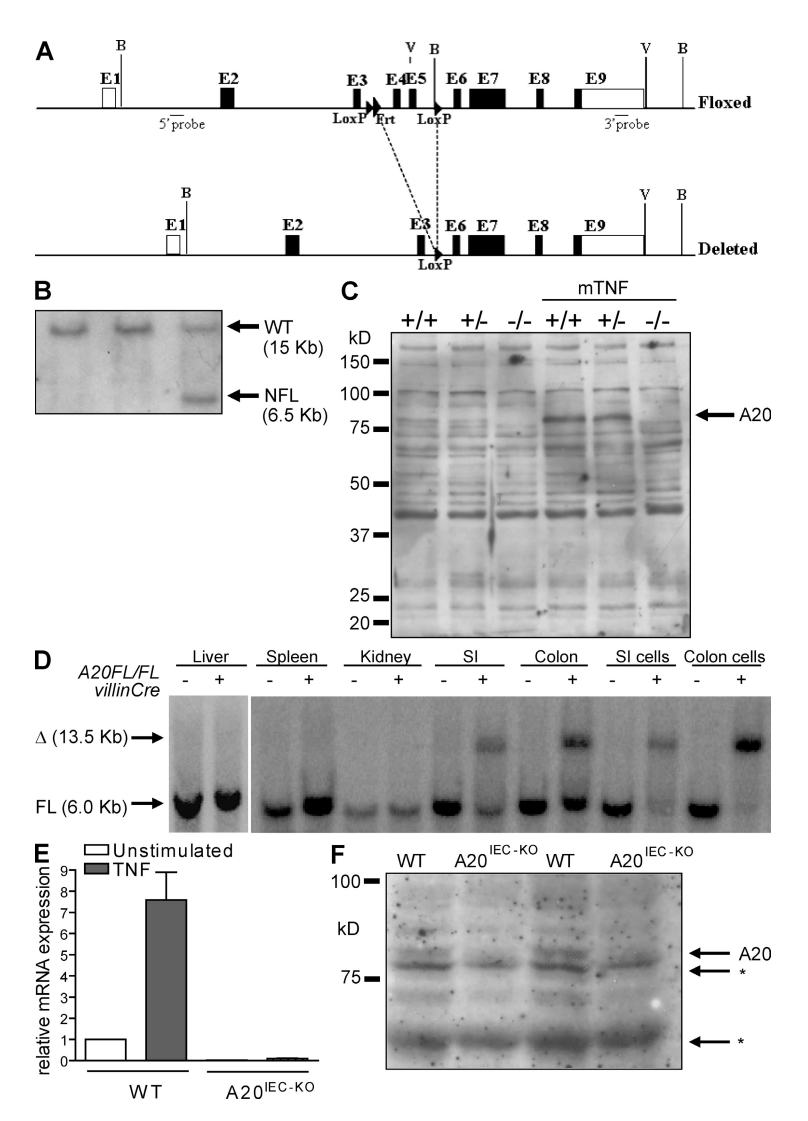
¹Department for Molecular Biomedical Research, VIB, B-9052 Ghent, Belgium

²Department of Biomedical Molecular Biology, Ghent University, B-9052 Ghent, Belgium

³Max Planck Institute of Biochemistry, D-82152 Martinsried, Germany

⁴Institute for Genetics, University of Cologne, D-50674 Cologne, Germany

^{© 2010} Vereecke et al. This article is distributed under the terms of an Attribution–Noncommercial–Share Alike–No Mirror Sites license for the first six months after the publication date (see http://www.rupress.org/terms). After six months it is available under a Creative Commons License (Attribution–Noncommercial–Share Alike 3.0 Unported license, as described at http://creativecommons.org/licenses/by-nc-sa/3.0/l.

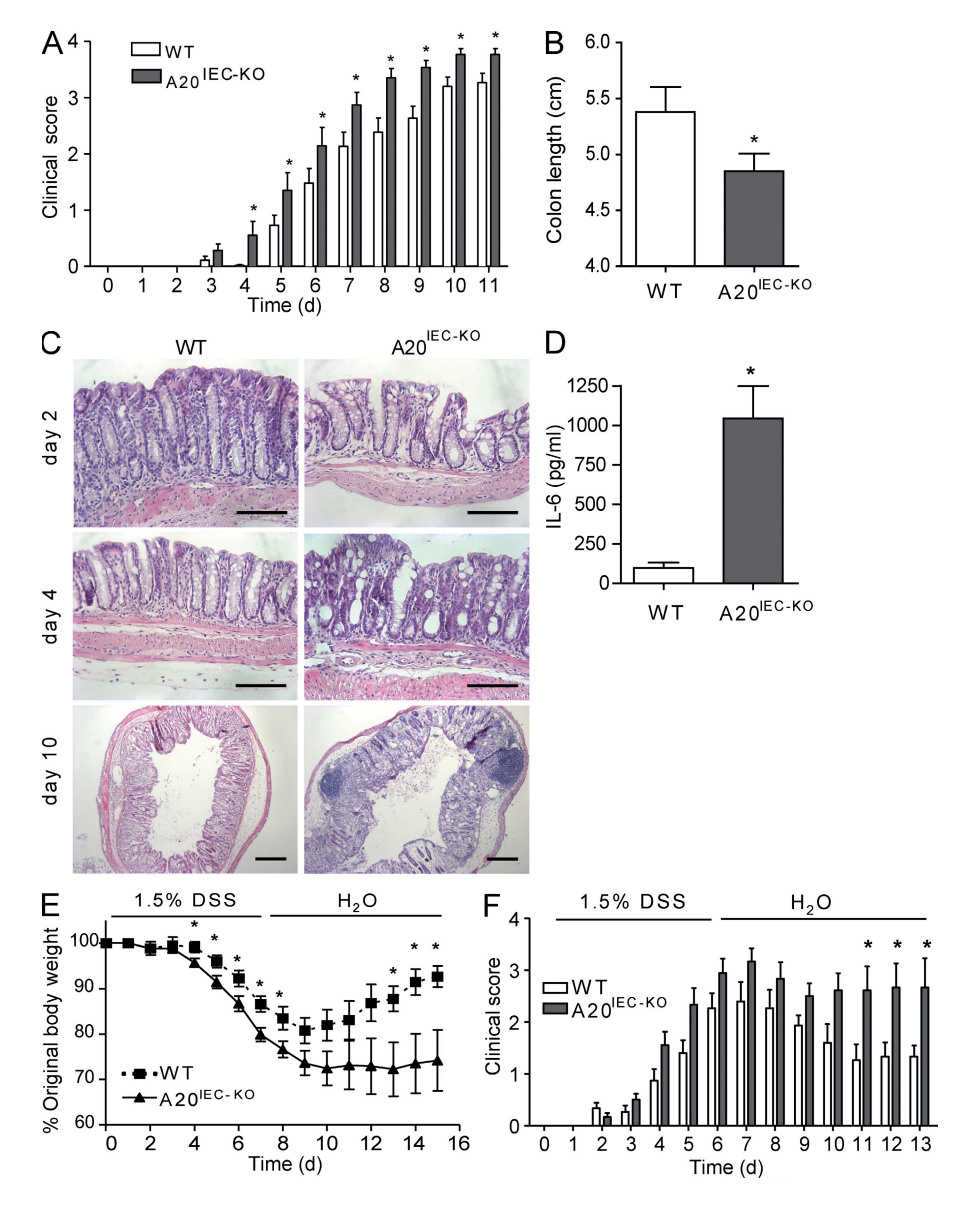


A20 is essential for the termination of NF-κB signaling in response to TNF and microbial products such as LPS and muramyl dipeptide (Boone et al., 2004; Hitotsumatsu et al., 2008), which trigger TLR4 and NOD2 (nucleotide-binding oligomerization domain-containing 2) receptors, respectively. Moreover, A20 also negatively regulates TNF-induced apoptosis (Opipari et al., 1992; Lee et al., 2000). Mice deficient for A20 are hypersensitive to TNF and die prematurely as a result of severe multiorgan inflammation and cachexia (Lee et al., 2000). Interestingly, A20 has recently been identified as a susceptibility locus for multiple immunopathologies (Vereecke et al., 2009). More specifically related to IBD, a recent genome-wide association study for seven major common diseases, undertaken in the British population by the Wellcome Trust Case Control Consortium (2007), identified A20 as a CD susceptibility gene. An earlier independent study on IBD-affected pairs of multiple families also associated mutations in a region of human chromosome 6q, containing the A20 locus, with the IBD phenotype (Barmada et al., 2004). Finally, mucosal biopsies from CD patients confirmed a consistent down-regulation of mucosal A20 expression in CD patients,

Figure 1. Generation and molecular analysis of A20^{IEC-KO} mice. (A) Targeting scheme. The diagram shows the loxPflanked (floxed) and deleted A20 alleles. The boxes indicate exons 1–9 (E1–E9). Restriction enzyme sites and the location of the probe used for Southern blot analysis are depicted. B, BamH1; V, EcoRV. LoxP and Frt sites are indicated by arrowheads. (B) Southern blot analysis on DNA from WT (+/+) and homologous recombinant (NFL/+) ES cells. (C) Western blot analysis for A20 expression in WT (+/+), heterozygous (+/-), and A20 knockout (-/-) primary MEFs either stimulated or not for 5 h with recombinant mouse TNF. (D) DNA isolated from various tissues of a A20FL/FL/Villin-Cre+ mouse and a control littermate (A20FL/FL/Villin-Cre-) was subjected to Southern blot analysis. Δ , deleted allele; FL, floxed allele; SI, small intestine. (E) Quantitative PCR measurement of A20 mRNA expression in purified IECs from A20^{IEC-KO} (n = 2) and control WT littermate mice (n = 2) 0 or 30 min after mouse TNF injection. Error bars represent SEM. (F) Western blot analysis for A20 expression in colonic epithelial cells from two individual A20^{IEC-KO} and control WT littermate mice. *, unspecific. Data are representative of two independent experiments.

which may hamper their ability to regulate pathological NF-κB activation induced by acute inflammatory responses (Arsenescu et al., 2008). Interestingly, single nucleotide polymorphisms in the *A20* region on 6q23.3 were recently also identified as a disease risk factor in celiac disease (Trynka et al., 2009). These studies, as well as the fact that mice genetically deficient in A20 develop multiorgan inflammation including severe intestinal inflammation (Lee et al., 2000), indicate that defective A20 expression or activity could be a risk factor for IBD. Previous studies showed that transfer of A20-deficient myeloid cells in WT irradiated mice elicits the spontaneous inflammatory phenotype as seen in full A20 knockout mice (Turer et al.,

2008). These data indicate that A20 expression in myeloid cells plays a key role in restricting proinflammatory signaling. However, whether A20 also has a role in stromal cells such as the intestinal epithelium remains unknown. There is multiple evidence that epithelial NF-kB preserves the integrity of the gut epithelial barrier and maintains immune homeostasis in the gut (Ben-Neriah and Schmidt-Supprian, 2007; Artis, 2008; Pasparakis, 2008). Epithelial-specific NF-κB deficiency in mice through conditional ablation of NF-kB essential modulator (NEMO) or both IkB kinase (IKK) 1 and IKK2 spontaneously led to enterocyte apoptosis and massive intestinal inflammation (Nenci et al., 2007). Similarly, mice with specific deletion of RelA in intestinal epithelial cells (IECs) exhibit increased susceptibility to chemically induced colitis (Steinbrecher et al., 2008). An important step in the inflammatory process in these NF-κBdeficient mice involves the sensitization of NF-kB-deficient epithelial cells to TNF-induced apoptosis, compromising epithelial integrity and allowing bacterial translocation into the mucosa, thus leading to recruitment of inflammatory immune cells and chronic inflammation (Nenci et al., 2007). The identity of



the NF-kB-regulated genes that control enterocyte survival in intestinal immune homeostasis or in a proinflammatory environment remains unknown. A20 is an NF-κB-dependent gene that is naturally expressed in mouse enterocytes as soon as the gut gets colonized by bacteria, a process which is initiated right after birth (Wang et al., 2009). We might, therefore, expect an important role for A20 in establishing NF-κB-mediated tolerance and epithelial protection against environmental and proinflammatory signals. However, the dual antiapoptotic and NF-κBinhibitory function of A20 imposes a real conundrum. On the one hand, A20 deficiency in the gut would increase the susceptibility of enterocytes to apoptosis, leading to the translocation of commensal bacteria and intestinal inflammation. On the other hand, and consistent with the previously reported key role of NF-kB in maintaining immune homeostasis in the gut (Ben-Neriah and Schmidt-Supprian, 2007; Nenci et al., 2007; Pasparakis, 2008; Steinbrecher et al., 2008), excessive NF-kB

Figure 2. Enterocyte expression of A20 is required for recovery of mice from acute DSS-induced inflammation.

(A) Clinical score of A20^{IEC-KO} mice (n = 18) and control littermates (WT, n = 20) treated with 1.5% DSS. (B) Colon length of A20IEC-KO mice (n = 18) and control littermates (WT, n = 20) after 10 d of 1.5% DSS treatment. (C) Hematoxylin and eosin (H&E) histology on DSS-treated A20^{IEC-KO} mice and control littermates (WT). Bars: (days 2 and 4) 100 μm; (day 10) 250 μm. (D) Serum IL-6 levels after 1.5% DSS treatment for 4 d. (E and F) Clinical score and body weight of A20^{IEC-KO} mice (n =6) and control littermates (WT, n = 5) treated for 6 d with 1.5% DSS followed by normal drinking water. Data in A-D are representative of three independent experiments. Experiments in E and F were performed two times. Error bars represent SEM. *, P < 0.05.

activation in A20-deficient enterocytes can be expected to be protective.

To study the role of A20 expression in IECs in intestinal immunity under normal and proinflammatory conditions, we generated A20 conditional knockout mice that are specifically deficient for A20 in IECs. IEC-specific A20 knockout (A20^{IEC-KO}) mice show increased susceptibility to dextran sodium sulphate (DSS)-induced colitis associated with increased sensitivity of IECs to apoptosis. A20^{IEC-KO} mice are also hypersensitive to normally sublethal doses of TNF, leading to enterocyte apoptosis and disintegration of the intestinal barrier. As a result, infiltrating

commensal bacteria initiate a systemic inflammatory response leading to death. These data indicate that A20 expression in the intestinal epithelium is a crucial antiapoptotic factor that mediates the protective effect of NF- κ B in IEC and determines susceptibility to IBD.

RESULTS

Generation and phenotypic analysis of A20^{IEC-KO} mice

We generated mice carrying a conditional A20 allele in which exons IV and V of the mouse A20 gene are flanked by LoxP sites (Fig. 1 A). This conditional A20 allele allows the tissue-specific inactivation of A20 through expression of Cre recombinase, as removal of exons IV and V results in an out-of-frame transcript. Correctly targeted homologous recombinant embryonic stem (ES) cell clones were identified by Southern blotting and used to generate chimeric mice that transmitted the targeted allele to their offspring (Fig. 1 B). Mice homozygous for the LoxP-flanked A20 allele (A20^{FL/FL})

JEM VOL. 207, July 5, 2010 1515

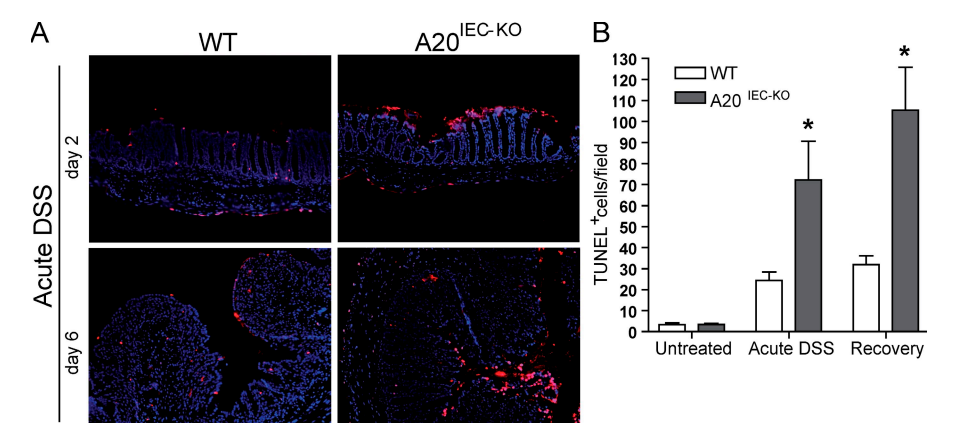
express normal levels of A20 and develop normally (Fig. S1). Deletion of the LoxP-flanked A20 alleles through expression of the Cre recombinase leads to a loss of A20 protein, as shown in mouse embryonic fibroblasts (MEFs; Fig. 1 C). Moreover, no alternative or shorter A20 protein can be detected in A20^{-/-} MEFs. To study the role of A20 in physiological maintenance of the IEC layer as well as its response to intestinal inflammation, we crossed the A20^{FL/FL} mice with a transgenic mouse line that expresses Cre under the control of the IEC-specific villin gene regulatory sequences (villin-Cre). The villin-Cre transgenic line targets all epithelial cell lineages of the distal small intestine, cecum, and colon, and expression mediates efficient Cre-mediated recombination in IECs starting before birth (Madison et al., 2002). A20^{IEC-KO} (A20^{FL/FL}/villin-Cre, A20^{IEC-KO}) mice were born showing normal Mendelian segregation and reached adulthood without any evidence of intestinal defects. To verify the tissue specificity of the A20^{IEC-KO}, we performed Southern blot analysis of DNA isolated from various tissues of a A20^{IEC-KO} mouse, showing efficient Cre-mediated recombination in intestinal tissue (colon and small intestine) and in purified IECs isolated

from colon and small intestine (Fig. 1 D). Recombination was not detected in any other tested tissues. In addition, quantitative real-time PCR on IEC mRNA and immunoblot analysis of IEC protein extracts revealed ablation of A20 in A20 $^{\rm IEC\text{-}KO}$ cells (Fig. 1, E and F).

A20 expression in IEC determines the susceptibility to experimental colitis

A20^{IEC-KO} mice look healthy, and phenotypic analysis of A20^{IEC-KO} mice up to the age of 12 mo revealed no pathological signs in the intestine. To further investigate whether A20 expression determines the susceptibility to IBD, A20^{IEC-KO} mice and control littermates were evaluated in an established model of DSS-induced colitis. Mice were subjected to 1.5% DSS in drinking water for 9 d and monitored daily for clinical pathology based on loss in body weight, stool consistency, and presence of fecal blood. Compared with control mice, A20^{IEC-KO} mice show increased susceptibility to DSS-induced colitis and develop more severe colitis symptoms, like gross rectal bleeding and diarrhea (Fig. 2 A). Colon shortening, a typical clinical feature of colonic inflammation, is much more pronounced

in A20^{IEC-KO} mice 10 d after DSS treatment (Fig. 2 B). Histological examination of the distal colon reveals increased mucosal damage, crypt loss, and immune cell infiltration in DSS-treated A20^{IEC-KO} mice compared with control littermates (Fig. 2 C). Inflammation was further assessed by quantifying the presence of IL-6 in serum. In contrast to untreated mice, which do not show inflammatory cytokine expression (not depicted), IL-6 was found to be significantly



A20^{IEC-KO}

D

125

100

A20 IEC-KO

Tolor

Tolor

A20 IEC-KO

Figure 3. A20 deficiency sensitizes IECs to DSS-induced apoptosis. (A) TUNEL staining on distal colon sections of A20^{IEC-KO} mice and control littermates (WT) after 2 and 6 d of 1.5% DSS treatment, and after 9 d during recovery (6 d of 1.5% DSS followed by normal drinking water). Bars, 150 µm. (B) Quantification of the number of TUNEL-positive cells/field from untreated and DSS-treated mice. Error bars represent SEM. *, P < 0.05. (C) Detection of BrdU incorporation on distal colon sections of A20^{IEC-KO} mice and control littermates (WT) after 6 d of 1.5% DSS treatment, and after 9 d during recovery (6 d of 1.5% DSS followed by normal drinking water). Bars: (day 4) 50 μm; (day 9) 250 μm. (D) Quantification of the number of BrdU-positive cells/ field from untreated and DSS-treated mice. Error bars represent SEM. Data are representative of three independent experiments.

Recovery

day 9

Recovery

С

Acute DSS

day 6

day 9

WT

higher in A20^{IEC-KO} mice then in controls after DSS treatment (Fig. 2 D).

To evaluate the ability of A20^{IEC-KO} mice to recover from DSS-induced epithelial damage, mice were put on 1.5% DSS for 6 d and were then put back on regular drinking water. Control mice display maximal clinical colitis on day 7, after which they recover and gain up to 90% of their original body weight (Fig. 2, E and F). A20^{IEC-KO} mice, however, are unable to cope with the initial DSS challenge and do not recover. All A20^{IEC-KO} mice continue to display severe signs of clinical colitis, they do not gain weight, and many of them (66%) die around day 12–13 after treatment (Fig. 2, E and F). The increased and sustained pathological response in A20^{IEC-KO} mice indicates an essential role for A20 in the termination of intestinal inflammation and the recovery from intestinal epithelial damage.

A20 protects IECs from apoptosis in experimental colitis

A20 has a dual NF-kB inhibitory and antiapoptotic effect (Coornaert et al., 2009). The increased susceptibility of A20^{IEC-KO} mice to DSS-induced colitis may therefore be explained by increased IEC apoptosis, allowing infiltration of commensal bacteria into the submucosa and the activation of several immune cells that built up a proinflammatory environment, leading to a further breakdown of the epithelial barrier. Therefore, we determined apoptosis in the intestinal epithelium of A20^{IEC-KO} and control littermate mice after DSS challenge by TUNEL staining. Compared with controls, A20^{IEC-KO} epithelium already showed much more TUNEL-positive cells after the start of DSS treatment (days 2-6) (Fig. 3, A and B), which is likely an underestimation because of the significant loss of IECs in A20^{IEC-KO} mice as a result of excessive mucosal damage. This difference in epithelial cell apoptosis between A20^{IEC-KO} and control littermate mice is even more pronounced during the recovery phase after putting mice back on regular

A 20 IEC-KO My D 88 -/
A 20 IEC-KO My D 88 -/
A 20 IEC-KO My D 88 -/
Time (d)

C 4

A 20 IEC-KO TNFRI -/
A 3 --
A 20 IEC-KO TNFRI -/
A 20 IEC-KO TNFRI -/
A 20 IEC-KO TNFRI -/
A 3 --
A 3 --
A 4 --
A 5 6 7 8 9 9

drinking water (day 9; Fig. 3, A and B). Although IECs from A20^{IEC-KO} mice are highly sensitive to apoptosis when exposed to DSS, the expression of different pro- or antiapoptotic genes (Bax, PUMA, Bcl2, BclXL, and XIAP) was not significantly changed in A20-deficient IECs compared with DSS-challenged control IECs (unpublished data).

Next to increased apoptosis, A20-deficient IECs may have an impaired capacity to restore the epithelial barrier after DSS-induced epithelial erosion as the result of a decreased proliferative response. However, similar numbers of BrdU-labeled cells were found in A20^{IEC-KO} and control epithelial cell layers of DSS-treated animals during acute DSS treatment (Fig. 3, C and D), excluding a difference in proliferation in the absence of A20. During recovery (after putting mice back on regular drinking water, day 9), however, a slight difference in the numbers of BrdU-labeled cells between both groups is observed (Fig. 3, C and D). This difference most probably results from the excessive mucosal damage and the significant loss of IECs in A20^{IEC-KO} mice. Indeed, mucosal areas with modest damage display similar numbers of BrdU-labeled cells compared with control areas.

MyD88 deficiency exacerbates, whereas TNF receptor (TNFR) 1 deficiency reduces experimental colitis in A20^{IEC-KO} mice

Because TLRs expressed on IECs are essential as sensors of commensal bacteria establishing intestinal homeostasis (Rakoff-Nahoum et al., 2004), A20 could be involved in this regulation in addition to its role as a protective factor against IEC apoptosis. To explore this possibility, we also analyzed the sensitivity of A20^{IEC-KO} mice to DSS-induced colitis in a MyD88-deficient background. As expected, double A20^{IEC-KO}MyD88-deficient mice are much more sensitive to DSS-induced colitis compared with control A20^{IEC-KO}MyD88 heterozygous mice (Fig. 4 A). These re-

sults suggest that, in addition to enhanced IEC apoptosis in the absence of A20, a defective TLR-mediated bacterial recognition in the absence of MyD88 contributes to DSS-induced intestinal inflammation and that both signals are happening in concert in conditions of A20 deficiency in IECs.

Figure 4. MyD88 deficiency sensitizes and TNFR1 deficiency reduces experimental colitis in A20^{IEC-KO} mice. (A) Clinical score of A20^{IEC-KO}MyD88-deficient mice (n=4) and control A20^{IEC-KO}MyD88 heterozygous mice (n=4) treated with 1.5% DSS. (B) Clinical score of double A20^{IEC-KO}MyD88-deficient mice (n=4) and single MyD88 knockout mice (n=4) treated with 1.5% DSS. (C) Clinical score of A20^{IEC-KO}TNFR1-deficient mice (n=10) and control A20^{IEC-KO}TNFR1 heterozygous mice (n=5) treated with 1.5% DSS. (D) Clinical score of double A20^{IEC-KO}TNFR1-deficient mice (n=10) and single TNFR1 knockout mice (n=7) treated with 1.5% DSS. Error bars represent SEM. *, P < 0.05. Data are representative of two independent experiments.

JEM VOL. 207, July 5, 2010

This is also strengthened by the fact that double A20^{IEC-KO-}MyD88-deficient mice are much more sensitive to DSS-induced inflammation than single MyD88-deficient mice (Fig. 4 B). Overall, it can be concluded from these results that both MyD88 and A20 play a nonredundant protective role in intestinal immune homeostasis.

TNF is one of the major proinflammatory cytokines contributing to the pathogenesis of CD in humans and experimental colitis in mice, and TNF-blocking agents have shown clinical efficiency in both patients and mice (Neurath et al., 1997; Targan et al., 1997). To investigate whether TNF signaling contributes to the development of colitis in DSS-treated A20^{IEC-KO} mice, we crossed them onto a TNFR1-deficient background. Double A20^{IEC-KO}TNFR1-deficient mice and control A20^{IEC-KO}TNFR1 heterozygous mice were subjected to DSS and monitored for clinical pathology. Compared with control mice, A20^{IEC-KO}TNFR1-deficient mice develop less severe colitis symptoms (Fig. 4 C), demonstrating that A20 restricts harmful TNFR1 signaling which contributes to disease pathogenesis in this model. Compared with TNFRI-deficient mice, double A20^{IEC-KO}TNFRI-deficient mice are more sensitive to DSS-induced colitis (Fig. 4 D), further suggesting that A20 also restricts the role of other receptors than TNFRI, such as TLRs and NLRs, in DSS-induced colitis. We can conclude that A20 acts as a major protective NF-kB response gene in the intestinal epithelium by restricting both proinflammatory and proapoptotic signaling pathways induced by TLR-MyD88 and TNFRI, respectively.

A20 deficiency in IEC increases TNF-induced damage of the intestinal epithelium and lethality

TNF may contribute to disease pathology by activating NF-κB and inflammation, as well as by inducing apoptosis of IECs, which causes loss of epithelial barrier integrity. Besides its well documented NF-kB inhibitory function, A20 also inhibits TNF-induced apoptosis (Opipari et al., 1992; Lee et al., 2000; Coornaert et al., 2009). We therefore evaluated the effect of A20 deficiency in IECs on TNF-induced pathology. For this, we injected A20^{IEC-KO} mice and control littermates with a normally sublethal dose of mouse TNF. In contrast to control mice, which all resist such a sublethal dose of TNF and only show a modest drop in body temperature 6-8 h after injection, A20^{IEC-KO} mice display typical symptoms associated with TNF toxicity, including hypothermia and severe diarrhea, already starting 2 h after injection. 5 h after TNF administration, all A20^{IEC-KO} mice showed a severe drop in body temperature (Fig. 5 A), and they died between 5 and 9 h after injection, whereas all control mice survived (Fig. 5 B). We further assessed inflammation in A20^{IEC-KO} mice by quantifying proinflammatory cytokine and chemokine production after TNF injection. A20^{IEC-KO} mice had higher levels of IL-6 and MCP-1 in circulation after TNF challenge than control littermate mice (Fig. 5 C). TNF toxicity in A20^{IEC-KO} mice involves TNFR1 signaling, as injecting human TNF, which only binds mouse TNFR1 and not mouse TNFR2 (Lewis et al., 1991), similarly induced lethality in A20^{IEC-KO} mice (Fig. 5 D).

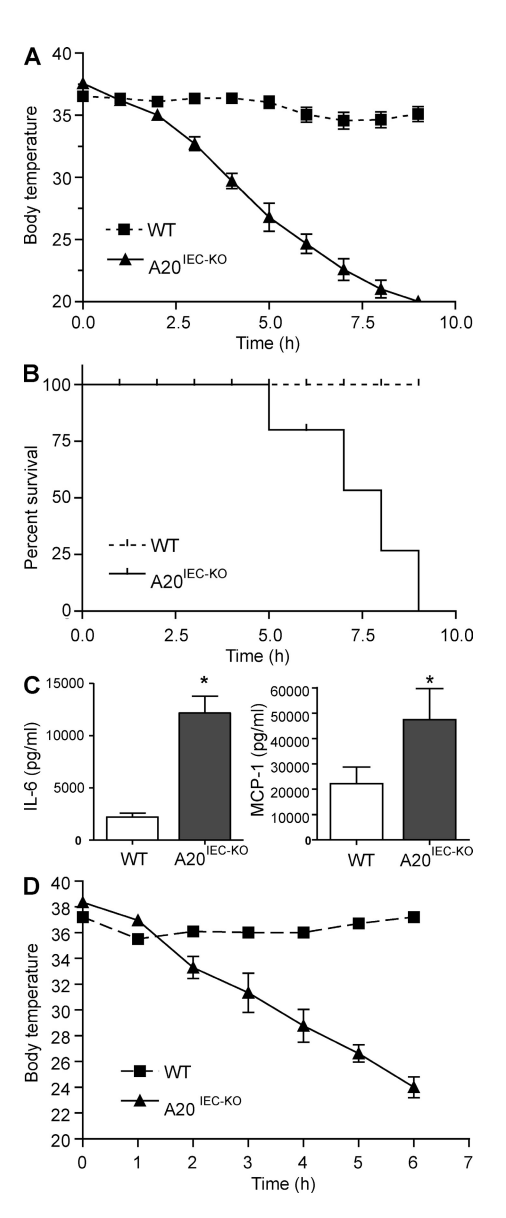


Figure 5. A20 deficiency in IECs sensitizes mice to TNF-induced toxicity. (A and B) Mice were injected i.p. with 5 μ g of recombinant mouse TNF. Body temperature (A) and survival (B) of A20^{IEC-KO} mice (n=8) and littermate control mice (WT; n=6). (C) Serum IL-6 and MCP-1 levels 4 h after mouse TNF injection. (D) Body temperature of A20^{IEC-KO} mice (n=6) and control littermate mice (n=6) after injection with 50 μ g of recombinant human TNF. Data are representative of three independent experiments. Error bars represent SEM. *, P < 0.05.

To investigate the TNF-induced tissue damage in A20^{IEC-KO} mice, parts of the intestine from control and A20^{IEC-KO} mice were removed and stained with hematoxylin/eosin for histological examination. Treatment with TNF resulted in severe damage of the jejunum and ileum of A20^{IEC-KO} mice, showing extensive epithelial destruction and a nearly complete loss of crypt-villus structure, which is in contrast to control littermates which maintain tissue integrity (Fig. 6 A). To investigate TNF-induced apoptosis at the cellular level, intestinal tissue sections were analyzed by TUNEL assay. In control mice

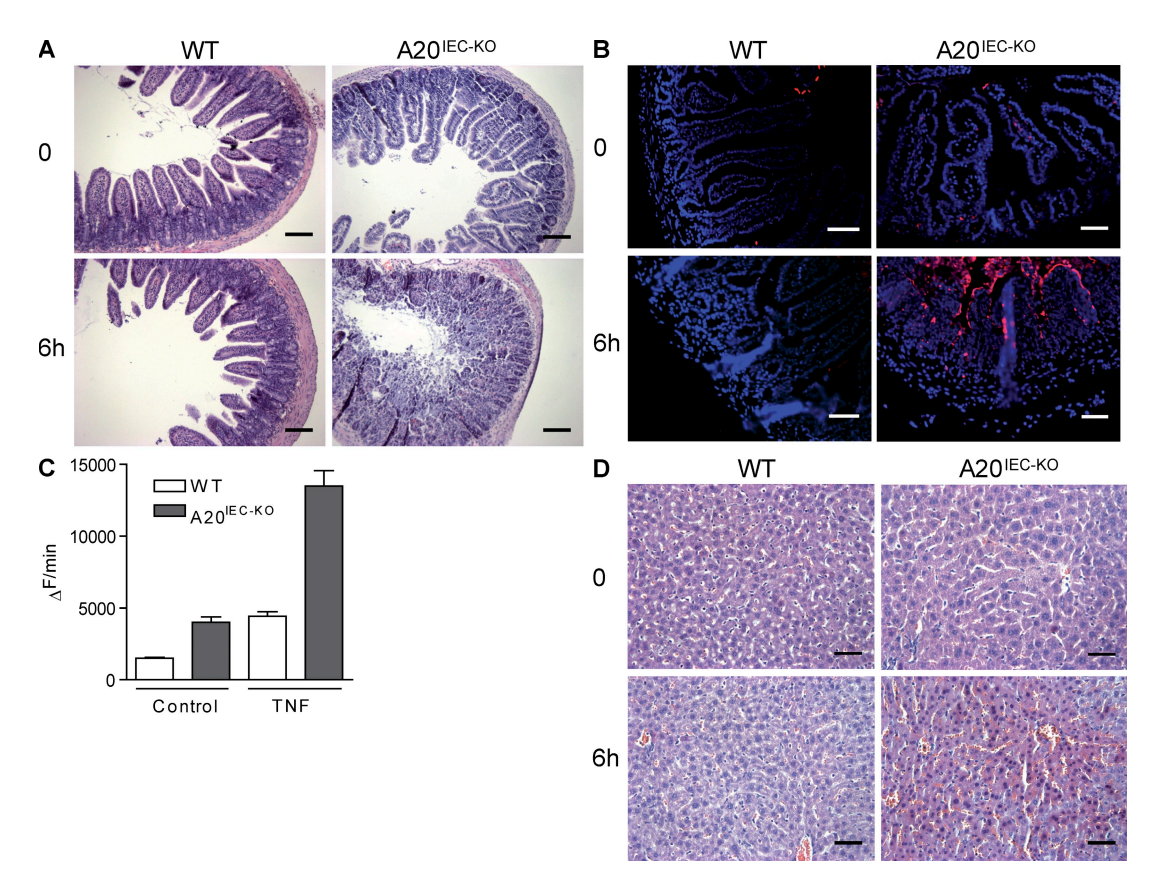


Figure 6. A20 deficiency in IECs sensitizes to TNF-induced damage of the small intestine and liver. (A) H&E histology on a section of the small intestine from A20^{IEC-KO} mice and control littermates (WT) 0 and 6 h after mouse TNF injection. Bars, 100 μm. (B) TUNEL staining on sections from small intestine 0 and 6 h after mouse TNF injection, staining apoptotic cells in red. Bars, 50 μm. (C) Caspase activity assayed on tissue homogenates of terminal ileum of A20^{IEC-KO} mice and WT littermates at 0 (control) and 90 min after mouse TNF injection. Error bars represent SEM. (D) H&E histology on liver samples from control (WT) and A20^{IEC-KO} mice 0 and 6 h after mouse TNF injection. Bars, 50 μm. Data are representative of two independent experiments.

treated with TNF, TUNEL staining was completely absent. In contrast, TNF-challenged A20^{IEC-KO} mice showed massive positive TUNEL staining, mainly at the epithelial cells lining the villi (Fig. 6 B; Fig. S2 A). Moreover, numerous apoptotic cells could be detected in the intestinal lumen. In contrast to the enhanced sensitivity of A20-deficient IECs to apoptosis, no differences in epithelial cell proliferation could be observed between A20^{IEC-KO} and control littermate mice (Fig. S2 B). To confirm IEC apoptosis in TNF-treated A20^{IEC-KO} mice, intestinal tissue homogenates were made and the extent of apoptosis was assessed by measuring caspase activity. PBS-injected A20^{IEC-KO} mice already show higher caspase activity then control littermates (Fig. 6 C). Moreover, the effect of TNF was much more pronounced in A20^{IEC-KO} mice, which is in agreement with the increase in apoptosis as observed in the TUNEL assay. Finally, to analyze whether A20 deficiency in the intestinal epithelium also induced histopathological changes in other tissues, we examined the liver of TNF-treated control and A20^{IEC-KO} mice. Interestingly, TNFtreated A20^{IEC-KO} mice not only show increased damage of the intestinal tissue but also of the liver (Fig. 6 D and Fig. S3), although A20^{IEC-KO} mice express normal A20 levels in this tissue (Fig. S4). This demonstrates that specific A20 deficiency

in the intestine can also affect the systemic effects of TNF on other tissues.

Commensal intestinal microbes contribute to TNF-induced lethality in A20^{IEC-KO} mice

As TNF induces massive epithelial destruction in A20^{IEC-KO} mice, infiltration of commensal bacteria may contribute to the lethal inflammatory shock observed in these mice. To determine to what extent commensal intestinal microbes contribute to epithelial damage and lethality in A20^{IEC-KO} mice, we treated these mice for 2 wk with a mix of broadspectrum antibiotics (ciprofloxacin, ampicillin, metronidazole, and vancomycin), which has been shown to substantially reduce the numbers of commensal bacteria in the intestine (unpublished data). Interestingly, antibiotics treatment completely protected A20^{IEC-KO} mice against the lethal effect of TNF up to 8 h after TNF injection (Fig. 7 A). A20^{IEC-KO} mice that are rescued from TNF-induced lethality by antibiotics still show massive epithelial destruction in the small intestine (Fig. 7 B), although epithelial damage is less severe than in TNF-treated mice that did not receive antibiotics (not depicted). This suggests that a mucosal cytokine burst initiated by bacterial infiltration contributes to further epithelial damage

JEM VOL. 207, July 5, 2010

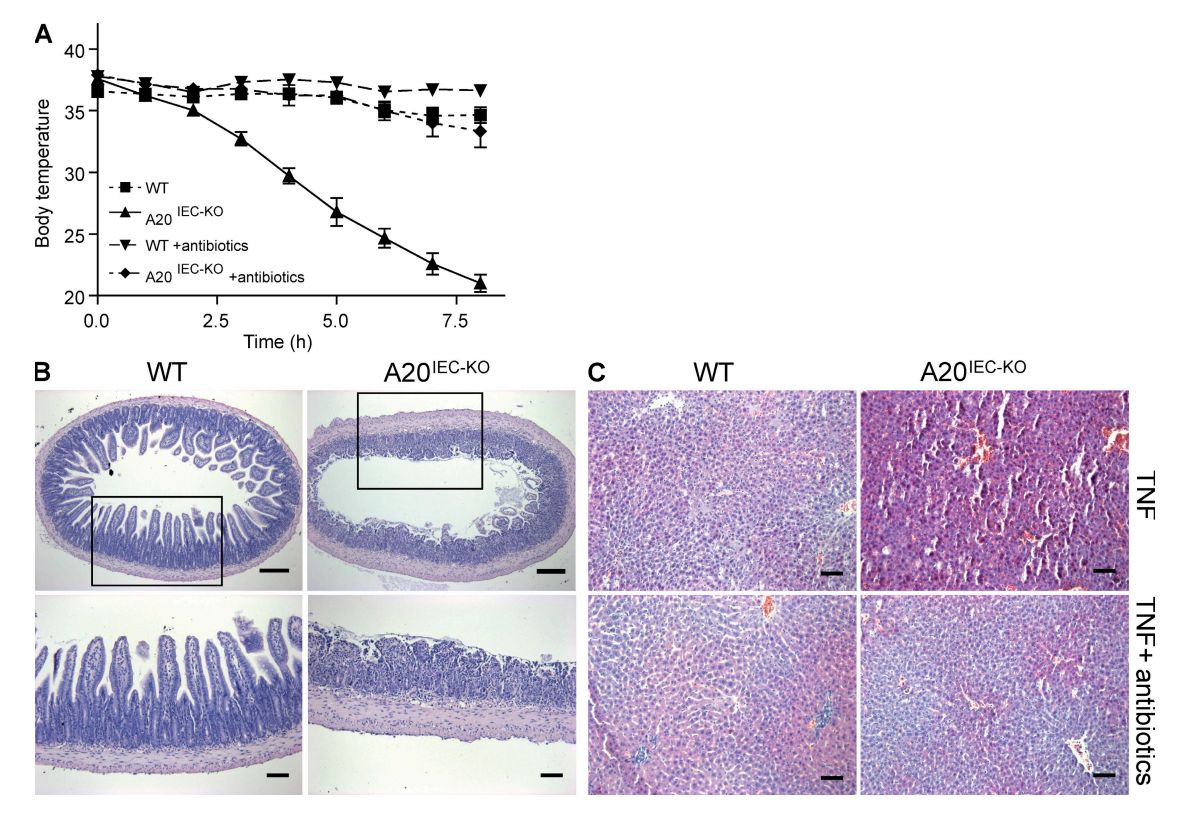


Figure 7. Commensal intestinal microbes contribute to TNF-induced toxicity in A20^{IEC-KO} mice. (A) Body temperature after mouse TNF challenge of A20^{IEC-KO} mice and control littermate mice (WT) either untreated (IEC-KO, n = 6; WT, n = 5) or treated (IEC-KO, n = 6; WT, n = 8) with broad-spectrum antibiotics. (B) H&E histology on sections from distal ileum 0 and 7 h after i.p. injection of mouse TNF in control (WT) and A20^{IEC-KO} mice treated with antibiotics. Bottom images are magnifications of rectangles in top images. Bars: (top) 100 μm; (bottom) 75 μm. (C) H&E histology on liver samples 0 and 7 h after TNF injection in control (WT) and A20^{IEC-KO} mice either untreated or treated with antibiotics. Bars, 75 μm. Data are representative of two independent experiments. Error bars represent SEM.

in the absence of A20. However, although intestinal epithelial damage in A20^{IEC-KO} mice is only slightly reduced by antibiotics treatment, TNF-induced liver damage is completely prevented (Fig. 7 C). Collectively, these data suggest that infiltration of commensal bacteria as a result of the TNF-mediated destruction of the epithelial barrier in A20^{IEC-KO} mice initiates a systemic inflammatory response, causing dramatic body temperature loss, severe liver damage, and cardiovascular collapse causing lethality.

DISCUSSION

In this paper, we have shown that the NF-κB-regulated gene A20 is a major protective factor in the intestinal epithelium. Specific deletion of A20 in enterocytes increased the susceptibility of mice to DSS-induced colitis and prevented the recovery from acute DSS-induced inflammation. We also demonstrated that A20 deficiency in enterocytes renders mice sensitive to TNF-induced lethal inflammation. TNF-induced lethality was mediated by an apoptotic effect of TNF on A20-deficient cells, leading to disruption of the epithelial barrier and infiltration of commensal bacteria that initiate a systemic inflammatory response.

A20 is well documented as an NF- κ B-responsive gene that plays a key role in the negative feedback regulation of NF- κ B

signaling (Coornaert et al., 2009). However, A20 is also recognized as a strong antiapoptotic factor (Opipari et al., 1992; Lee et al., 2000). This may seem contradictory, as NF-kB is important for cytoprotection by inducing the expression of antiapoptotic genes and cell cycle regulators (Luo et al., 2005). NF-κB inhibition is therefore often sensitizing toward cell death. Because enterocytes from A20^{IEC-KO} mice are highly sensitive to TNF-induced apoptosis, the antiapoptotic effect of A20 seems to be dominant to the cell death-sensitizing effect of NF-kB inhibition. Moreover, this would suggest that the antiapoptotic function of A20 is sufficient for its protective effect against sublethal TNF doses. We cannot exclude, however, that an additional antiinflammatory effect of NF-κB inhibition by A20 also contributes to its protective function. The hypersensitivity of A20^{IEC-KO} mice to DSS-induced acute colitis is consistent with the important role of NF-kB in IBD. It was previously reported that defective NF-κB activity in intestinal epithelium as a result of enterocyte-specific ablation of the regulatory subunit of the IKK complex NEMO, as well as of enterocyte-specific RelA deficiency, causes spontaneous colitis (Nenci et al., 2007; Steinbrecher et al., 2008). It can be hypothesized that this phenotype is partly caused by the defective NF-κB-dependent expression of A20. However, in contrast to NEMO- or RelA-deficient mice, A20IEC-KO mice do not

develop spontaneous intestinal inflammation, at least at young age, indicating that enterocyte A20 expression is dispensable for normal intestinal immune homeostasis.

TNF is one of the major proinflammatory cytokines contributing to the malignancy of IBD, and TNF blockade is an effective therapy for IBD patients (Targan et al., 1997). By inducing enterocyte apoptosis, aberrant TNF production may cause loss of epithelial barrier integrity, which is considered an early step in the pathogenesis of IBD. Our data show that in the absence of A20, enterocytes become hypersensitive to TNF-induced apoptosis, compromising epithelial integrity. Interestingly, A20 deficiency not only sensitizes mice to mouse TNF but also to human TNF, which is hardly toxic in WT mice (Ameloot et al., 2002). Therefore, our A20^{IEC-KO} mice may be a useful tool to study human TNF-targeting therapeutic strategies. Moreover, although mouse TNF binds both TNFR1 and TNFR2, human TNF only binds TNFR1 (Lewis et al., 1991), demonstrating that intestinal damage in A20^{IEC-KO} mice is mediated by TNFR1. The exact molecular mechanism by which A20 prevents TNF-induced apoptosis is still unclear. The ubiquitin-editing function of A20 has been shown to be responsible for its NF-kB inhibitory properties (Wertz et al., 2004; Heyninck and Beyaert, 2005), and several NF-κB signaling proteins can be deubiquitinated by A20 (Coornaert et al., 2009). Death receptor ligation was recently shown to induce polyubiquitination of the apoptosis signaling protein caspase-8, which led to the binding of the ubiquitin-binding protein p62/sequestosome-1, caspase-8 aggregation, and commitment to cell death (Jin et al., 2009). Interestingly, caspase-8 polyubiquitination could be reversed by A20, suggesting a possible antiapoptotic mechanism.

TNF-induced disruption of the intestinal epithelial barrier can be expected to allow mucosal infiltration of commensal bacteria, resulting in immune cell recruitment and activation. This would then result in the expression of several proinflammatory mediators, including TNF, which imposes further epithelial damage and complete epithelial barrier destruction. Ultimately, this allows bacteria to get in circulation and induce a systemic inflammatory response syndrome that is characterized by liver damage, severe hypotension, and death. The fact that we could inhibit TNF-induced lethality and liver damage in $A20^{\text{IEC-KO}}$ mice with antibiotics confirms a key role for commensal bacteria in TNF toxicity. It should be mentioned that treatment with antibiotics only slightly decreased TNFinduced intestinal epithelial damage in A20^{IEC-KO} mice, demonstrating that bacteria themselves are not responsible for enterocyte apoptosis. Previous studies showed that transfer of A20-deficient myeloid cells in irradiated WT mice induces multiorgan inflammation, as seen in full A20 knockout mice (Turer et al., 2008). These myeloid cell-transplanted mice are also completely protected with antibiotics or when bred onto a MyD88-negative background, demonstrating that A20 expression in myeloid cells is critical in restricting homeostatic TLR-mediated immune responses to intestinal commensal bacteria (Turer et al., 2008). Our data show that A20 also has a prominent role in stromal cells such as the intestinal epithelium. However, A20's primary function here is not to restrict MyD88-dependent proinflammatory signaling because these mice do not develop spontaneous inflammation in response to commensal bacteria but, rather, to control a cellular protection system once local intestinal inflammation is initiated. In such inflammatory conditions, A20 ensures maintenance of the epithelial barrier integrity by protecting cells from TNF-induced apoptosis.

In conclusion, because unrestrained activation of the immune system directed against the intestinal commensal microflora resulting in uncontrolled proinflammatory cytokine production is believed to play a key role in the development and progression of IBD (Round and Mazmanian, 2009), the present study further demonstrates that defects in the NFκB-dependent expression and function of A20 might play an important role in the development and progression of IBD. Although A20 expression in enterocytes is largely dispensable for normal intestinal tissue homeostasis, A20 has an essential protective role in conditions of intestinal injury and inflammation. These data also further support recent genome-wide association studies that identified A20 as a susceptibility locus for CD (Wellcome Trust Case Control Consortium, 2007; Arsenescu et al., 2008; Trynka et al., 2009) and other autoimmune diseases (Vereecke et al., 2009), implicating A20 as an interesting therapeutic target.

MATERIALS AND METHODS

Generation of IEC-specific knockout mice. To generate a conditional A20 allele, we prepared a targeting vector to flank exons IV and V of A20 with two LoxP sites. An Frt site-flanked cassette, containing a neo gene, was placed into the third intron of the A20 gene. A 4.0-kb fragment was used as 5' homology region, a 2-kb fragment was placed between the two LoxP sites, and a 4.0-kb fragment was used as 3' homology region. The targeting vector was linearized and transfected into Bruce-4 ES cells derived from C57BL/6 mice (Köntgen and Stewart, 1993) as previously described (Schmidt-Supprian et al., 2000). The targeted ES cell clone was injected into 3.5-d blastocysts and transferred to the uteri of pseudopregnant foster mothers. Male chimeras were mated with C57BL/6 females to obtain germline transmission of the A20 floxed allele (still containing the neomycine selection cassette; A20NFL). The Frt-flanked neomycin cassette was removed by crossing A20NFL mice with an Flp-deleter strain (Rodríguez et al., 2000) generating an A20 floxed allele (A20FL). A20+/- mice were generated by crossing chimeras transmitting the A20NFL genotype with Cre-deleter mice. MEFs were prepared from embryonic day 13.5 A $20^{+/+}$, A $20^{+/-}$, and A $20^{-/-}$ embryos. A $20^{FL/FL}$ mice were crossed to Villin-Cre transgenic mice (Madison et al., 2002; gift from D. Gumucio and B. Madison, University of Michigan Medical School, Ann Arbor, MI) to generate A20^{IEC-KO}. All experiments were performed on mice backcrossed into the C57BL/6 genetic background for at least five generations. Mice were housed in individually ventilated cages at the VIB Department of Molecular Biomedical Research in either specific pathogen-free or conventional animal facilities. All experiments on mice were conducted according to institutional, national, and European animal regulations. Animal protocols were approved by the ethics committee of Ghent University.

Southern and Western blot analysis. For ES cell selection, 10 μg of genomic DNA was digested with BamHI to differentiate between 15.0- and 6.5-kb fragments for the WT and A20^NFL alleles, respectively. To differentiate between A20^FL and A20^IEC-KO alleles, genomic DNA was digested with BamHI yielding 6.5- and 13.5-kb fragments, respectively. DNA was separated on agarose gels and transferred to nitrocellulose. Hybridization was performed with $^{32}\text{P-labeled}$ probe. Protein lysates were prepared from MEF,

JEM VOL. 207, July 5, 2010 1521

liver, or IEC samples, separated by SDS-PAGE (PAGE), transferred to nitrocellulose, and analyzed by immunoblotting. A20 was detected with rabbit polyclonal anti-A20 as primary antibody and anti-rabbit Ig-HRP (GE Healthcare) as secondary antibody. For the generation of anti-A20, rabbits were immunized with purified A20 OTU domain (gift from D. Komander, Medical Research Council Laboratory of Molecular Biology, Cambridge, England, UK) protein in TiterMax Gold and subsequently boosted five times with A20 OTU domain protein in Freund's adjuvant.

Proliferation and apoptosis assays. Proliferation was analyzed by microscopy after i.p. injection of 1 mg BrdU 2 h before sacrifice, using a BrdU in situ detection kit (BD). Apoptosis was analyzed by fluorescence microscopy using an in situ cell death detection kit (Roche). Five random optical fields were taken, and the results are presented as mean \pm SEM. Caspase activity was measured by incubation of 25 μg of tissue homogenate with 50 μM acetyl-Asp-Glu-Val-Asp-aminomethylcoumarin (Peptide Institute, Osaka, Japan) in 150 μl of cell-free system buffer (10 mM Hepes–NaOH, pH 7.4, 220 mM mannitol, 68 mM sucrose, 2 mM NaCl, 2.5 mM KH₂PO₄, 0.5 mM EGTA, 2 mM MgCl₂, 5 mM pyruvate, 0.1 mM PMSF, and 1 mM dithiothreitol). The release of fluorescent 7-amino-4-methylcoumarin was measured for 50 min at 2-min intervals by fluorospectrometry at 360 nm excitation and 480 nm emission wavelength, and the maximal rate of increase in fluorescence was calculated (Δfluorescence/min; Cytofluor; PerSeptive Biosystems).

In vivo TNF toxicity. Mice were injected i.p. with a sublethal dose of mouse or human TNF (5 μg of mouse [m] TNF/20-g mouse; 50 μg of human [h] TNF/20-g mouse). *E. wli*–derived recombinant mTNF had a specific activity of 9.46×10^7 IU/mg, and hTNF had a specific activity of 3×10^7 IU/mg. Both were produced and purified to homogeneity in our laboratory, and endotoxin levels did not exceed 1 ng/mg of protein. Body temperature and survival were monitored every hour, and blood was collected by retroorbital bleeding for cytokine analysis. In a separate experiment, mice were euthanized after 2 and 4 h for histological analysis and caspase activity assays.

Depletion of commensal intestinal bacteria. For antibiotic-mediated depletion of commensal bacteria, mice were treated with 200 mg/liter ciprofloxacin (Sigma-Aldrich), 1 g/liter ampicillin (Sigma-Aldrich), 1 g/liter metronidazole (Sigma-Aldrich), and 500 mg/liter vancomycin (Labconsult) in drinking water. After 2 wk, the presence of colonic microflora was determined by culturing fecal samples in both brain heart infusion (BD) and thioglycollate medium (Sigma-Aldrich).

Induction of DSS-induced colitis and clinical score. Female 8-12-wkold A20^{IEC-KO} and littermate WT controls were used in DSS-induced colitis experiments. Acute colitis was induced by addition of 1.5% DSS (36-50 kD; MP Biomedicals) to the drinking water for 9 or 6 d followed by regular distilled water. Body weight, occult or gross blood lost per rectum, and stool consistency were determined daily during the colitis experiment. Fecal blood was determined using Hemoccult SENSA (Beckman Coulter) analysis. The baseline clinical score was determined on day 0. In brief, no weight loss was scored as 0, weight loss of 1–5% from baseline as 1, 5–10% as 2, 10–20% as 3, and >20% as 4. For bleeding, a score of 0 was assigned for no blood, 2 for positive hemoccult, and 4 for gross bleeding. For stool consistency, a score of 0 was assigned for well-formed pellets, pasty and semiformed stools were scored as 2, and liquid stools as 4. These scores were added together and divided by three, resulting in a total clinical score ranging from 0 (healthy) to 4 (maximal colitis). To eliminate any diagnostic bias, mice were scored blindly.

Histological scoring. Postmortem, the entire colon was removed from cecum to anus, and the colon length was measured as a marker for inflammation.

Isolation of IECs. IECs were isolated as previously described (Nenci et al., 2007). In brief, small intestines or colons were dissected and flushed with a solution containing 154 mM NaCl and 1 mM DTT to remove fecal con-

tents. The intestinal segments were ligated, filled with PBS, and incubated in PBS at 37°C. After 15 min, PBS was substituted with PBS supplemented with 1.5 mM EDTA and 0.5 mM DTT. After 30 min at 37°C, one ligature was removed and contents were collected. These recovered cells were washed twice in PBS by centrifugation at 1,300 rpm for 5 min and were used for preparation of RNA or protein extracts.

Quantitative real-time PCR. Total RNA was isolated from purified IECs using the Aurum Total RNA Mini kit (Bio-Rad Laboratories) before cDNA synthesis using the iScript cDNA synthesis kit (Bio-Rad Laboratories) according to the manufacturer's instructions. 10 ng cDNA was used for quantitative PCR in a total volume of 10 μl with LightCycler 480 SYBR Green I Master Mix (Roche) and specific primers on a LightCycler 480 (Roche). Real-time PCR reactions were performed in triplicates. The following mouse-specific primers were used: A20 forward, 5'-AAACCAATGGTGATGGAAACTG-3'; A20 reverse, 5'-GTTGTCCCATTCGTCATTCC-3'; ubiquitin forward, 5'-AGGTCAAACAGGAAGACAGACGTA-3'; and ubiquitin reverse, 5'-TCACACCCAAGAACAAGCACA-3'.

Statistics. Results are expressed as the mean \pm SEM. Statistical significance between experimental groups was assessed using an unpaired two-sample Student's t test.

Online supplemental material. Fig. S1 shows normal A20 expression in A20^{FL} mice. Fig. S2 shows the number of apoptotic IECs and the number of proliferating IECs after TNF treatment. Fig. S3 shows AST and ALT levels in serum after TNF treatment. Fig. S4 shows normal A20 expression in liver from A20^{IEC-KO} mice.

We are grateful to Dr. Deborah Gumucio and Dr. Blair Madison for donating the Villin-Cre transgenic mouse, and to David Komander for kindly providing purified A20 OTU domain. We thank Tino Hochepied for transgenic services, and Pieter Rottiers, Janneke Samsom, Anje Cauwels, Claude Libert, and Filip Van Hauwermeiren for helpful discussions and suggestions. We are grateful to Dimitri Huyghebaert, Laetitia Bellen, and Carine Van Laere for animal care.

L. Vereecke is a PhD fellow with the Instituut voor Innovatie door Wetenschap en Technologie (IWT), C. Mc Guire is a PhD fellow with the Fonds voor Wetenschappelijk Onderzoek-Vlaanderen (FWO), and G. van Loo is a postdoctoral researcher with the FWO. G. van Loo is also supported by a Marie Curie Reintegration Grant from the sixth EU Framework Program (FP6-ERG-2005-031063) and an FWO Odysseus Grant. Work in the authors' laboratory is further supported by research grants from the Interuniversity Attraction Poles program (IAP6/18), the FWO, the Belgian Foundation against Cancer, the Strategic Basis Research program of the IWT, the Centrum voor Gezwelziekten, and the Concerted Research Actions (GOA) and Group-ID MRP of the Ghent University.

The authors declare no competing financial interests.

Submitted: 19 November 2009 Accepted: 5 May 2010

REFERENCES

Ameloot, P., N. Takahashi, B. Everaerdt, J. Hostens, H.P. Eugster, W. Fiers, and P. Brouckaert. 2002. Bioavailability of recombinant tumor necrosis factor determines its lethality in mice. Eur. J. Immunol. 32:2759–2765. doi:10.1002/1521-4141(2002010)32:10<2759::AID-IMMU2759>3.0 .CO;2-L

Arsenescu, R., M.E. Bruno, E.W. Rogier, A.T. Stefka, A.E. McMahan, T.B. Wright, M.S. Nasser, W.J. de Villiers, and C.S. Kaetzel. 2008. Signature biomarkers in Crohn's disease: toward a molecular classification. *Mucosal Immunol*. 1:399–411. doi:10.1038/mi.2008.32

Artis, D. 2008. Epithelial-cell recognition of commensal bacteria and maintenance of immune homeostasis in the gut. Nat. Rev. Immunol. 8:411–420. doi:10.1038/nri2316

Barmada, M.M., S.R. Brant, D.L. Nicolae, J.P. Achkar, C.I. Panhuysen, T.M. Bayless, J.H. Cho, and R.H. Duerr. 2004. A genome scan in 260 inflammatory bowel disease-affected relative pairs. *Inflamm. Bowel Dis.* 10:15–22. doi:10.1097/00054725-200401000-00002

- Baumgart, D.C., and S.R. Carding. 2007. Inflammatory bowel disease: cause and immunobiology. *Lancet*. 369:1627–1640. doi:10.1016/S0140-6736(07)60750-8
- Ben-Neriah, Y., and M. Schmidt-Supprian. 2007. Epithelial NF-kappaB maintains host gut microflora homeostasis. Nat. Immunol. 8:479–481. doi:10.1038/ni0507-479
- Boone, D.L., E.E. Turer, E.G. Lee, R.C. Ahmad, M.T. Wheeler, C. Tsui, P. Hurley, M. Chien, S. Chai, O. Hitotsumatsu, et al. 2004. The ubiquitin-modifying enzyme A20 is required for termination of Toll-like receptor responses. *Nat. Immunol.* 5:1052–1060. doi:10.1038/ni1110
- Coornaert, B., I. Carpentier, and R. Beyaert. 2009. A20: central gate-keeper in inflammation and immunity. *J. Biol. Chem.* 284:8217–8221. doi:10.1074/jbc.R800032200
- Heyninck, K., and R. Beyaert. 2005. A20 inhibits NF-kappaB activation by dual ubiquitin-editing functions. Trends Biochem. Sci. 30:1–4. doi:10.1016/j.tibs.2004.11.001
- Hitotsumatsu, O., R.C. Ahmad, R. Tavares, M. Wang, D. Philpott, E.E. Turer, B.L. Lee, N. Shiffin, R. Advincula, B.A. Malynn, et al. 2008. The ubiquitin-editing enzyme A20 restricts nucleotide-binding oligomerization domain containing 2-triggered signals. *Immunity*. 28:381–390. doi:10.1016/j.immuni.2008.02.002
- Jin, Z., Y. Li, R. Pitti, D. Lawrence, V.C. Pham, J.R. Lill, and A. Ashkenazi. 2009. Cullin3-based polyubiquitination and p62-dependent aggregation of caspase-8 mediate extrinsic apoptosis signaling. *Cell.* 137:721–735. doi:10.1016/j.cell.2009.03.015
- Köntgen, F., and C.L. Stewart. 1993. Simple screening procedure to detect gene targeting events in embryonic stem cells. *Methods Enzymol*. 225:878–890. doi:10.1016/0076-6879(93)25055-7
- Lee, E.G., D.L. Boone, S. Chai, S.L. Libby, M. Chien, J.P. Lodolce, and A. Ma. 2000. Failure to regulate TNF-induced NF-kappaB and cell death responses in A20-deficient mice. *Science*. 289:2350–2354. doi:10.1126/science.289.5488.2350
- Lewis, M., L.A. Tartaglia, A. Lee, G.L. Bennett, G.C. Rice, G.H. Wong, E.Y. Chen, and D.V. Goeddel. 1991. Cloning and expression of cDNAs for two distinct murine tumor necrosis factor receptors demonstrate one receptor is species specific. *Proc. Natl. Acad. Sci. USA*. 88:2830–2834. doi:10.1073/pnas.88.7.2830
- Luo, J.L., H. Kamata, and M. Karin. 2005. The anti-death machinery in IKK/NF-kappaB signaling. J. Clin. Immunol. 25:541–550. doi:10.1007/ s10875-005-8217-6
- Madison, B.B., L. Dunbar, X.T. Qiao, K. Braunstein, E. Braunstein, and D.L. Gumucio. 2002. Cis elements of the villin gene control expression in restricted domains of the vertical (crypt) and horizontal (duodenum, cecum) axes of the intestine. J. Biol. Chem. 277:33275–33283. doi:10.1074/jbc.M204935200
- Nenci, A., C. Becker, A. Wullaert, R. Gareus, G. van Loo, S. Danese, M. Huth, A. Nikolaev, C. Neufert, B. Madison, et al. 2007. Epithelial NEMO links innate immunity to chronic intestinal inflammation. *Nature*. 446:557–561. doi:10.1038/nature05698
- Neurath, M.F., I. Fuss, M. Pasparakis, L. Alexopoulou, S. Haralambous, K.H. Meyer zum Büschenfelde, W. Strober, and G. Kollias. 1997. Predominant pathogenic role of tumor necrosis factor in experimental colitis in mice. *Eur. J. Immunol.* 27:1743–1750. doi:10.1002/eji.1830270722
- Opipari, A.W. Jr., H.M. Hu, R. Yabkowitz, and V.M. Dixit. 1992. The A20 zinc finger protein protects cells from tumor necrosis factor cytotoxicity. J. Biol. Chem. 267:12424–12427.

- Pasparakis, M. 2008. IKK/NF-kappaB signaling in intestinal epithelial cells controls immune homeostasis in the gut. *Mucosal Immunol*. 1:S54–S57. doi:10.1038/mi.2008.53
- Podolsky, D.K. 2002. Inflammatory bowel disease. N. Engl. J. Med. 347:417–429. doi:10.1056/NEJMra020831
- Rakoff-Nahoum, S., J. Paglino, F. Eslami-Varzaneh, S. Edberg, and R. Medzhitov. 2004. Recognition of commensal microflora by toll-like receptors is required for intestinal homeostasis. *Cell.* 118:229–241. doi:10.1016/j.cell.2004.07.002
- Rakoff-Nahoum, S., L. Hao, and R. Medzhitov. 2006. Role of toll-like receptors in spontaneous commensal-dependent colitis. *Immunity*. 25:319–329. doi:10.1016/j.immuni.2006.06.010
- Renner, F., and M.L. Schmitz. 2009. Autoregulatory feedback loops terminating the NF-kappaB response. Trends Biochem. Sci. 34:128–135. doi:10.1016/j.tibs.2008.12.003
- Rodríguez, C.I., F. Buchholz, J. Galloway, R. Sequerra, J. Kasper, R. Ayala, A.F. Stewart, and S.M. Dymecki. 2000. High-efficiency deleter mice show that FLPe is an alternative to Cre-loxP. *Nat. Genet.* 25:139–140. doi:10.1038/75973
- Round, J.L., and S.K. Mazmanian. 2009. The gut microbiota shapes intestinal immune responses during health and disease. *Nat. Rev. Immunol*. 9:313–323. doi:10.1038/nri2515
- Schmidt-Supprian, M., W. Bloch, G. Courtois, K. Addicks, A. Israël, K. Rajewsky, and M. Pasparakis. 2000. NEMO/IKK gamma-deficient mice model incontinentia pigmenti. Mol. Cell. 5:981–992. doi:10.1016/S1097-2765(00)80263-4
- Steinbrecher, K.A., E. Harmel-Laws, R. Sitcheran, and A.S. Baldwin. 2008. Loss of epithelial RelA results in deregulated intestinal proliferative/apoptotic homeostasis and susceptibility to inflammation. J. Immunol. 180:2588–2599.
- Targan, S.R., S.B. Hanauer, S.J. van Deventer, L. Mayer, D.H. Present, T. Braakman, K.L. DeWoody, T.F. Schaible, and P.J. Rutgeerts. 1997. A short-term study of chimeric monoclonal antibody cA2 to tumor necrosis factor alpha for Crohn's disease. Crohn's Disease cA2 Study Group. N. Engl. J. Med. 337:1029–1035. doi:10.1056/NEJM199710093371502
- Trynka, G., A. Zhernakova, J. Romanos, L. Franke, K.A. Hunt, G. Turner, M. Bruinenberg, G.A. Heap, M. Platteel, A.W. Ryan, et al. 2009. Coeliac disease-associated risk variants in TNFAIP3 and REL implicate altered NF-kappaB signalling. Gut. 58:1078–1083. doi:10.1136/gut.2008.169052
- Turer, E.E., R.M. Tavares, E. Mortier, O. Hitotsumatsu, R. Advincula, B. Lee, N. Shifrin, B.A. Malynn, and A. Ma. 2008. Homeostatic MyD88-dependent signals cause lethal inflamMation in the absence of A20. *J. Exp. Med.* 205:451–464. doi:10.1084/jem.20071108
- Vereecke, L., R. Beyaert, and G. van Loo. 2009. The ubiquitin-editing enzyme A20 (TNFAIP3) is a central regulator of immunopathology. *Trends Immunol*. 30:383–391. doi:10.1016/j.it.2009.05.007
- Wang, J., Y. Ouyang, Y. Guner, H.R. Ford, and A.V. Grishin. 2009. Ubiquitin-editing enzyme A20 promotes tolerance to lipopolysaccharide in enterocytes. J. Immunol. 183:1384–1392. doi:10.4049/jimmunol.0803987
- Wellcome Trust Case Control Consortium. 2007. Genome-wide association study of 14,000 cases of seven common diseases and 3,000 shared controls. Nature. 447:661–678. doi:10.1038/nature05911
- Wertz, I.E., K.M. O'Rourke, H. Zhou, M. Eby, L. Aravind, S. Seshagiri, P. Wu, C. Wiesmann, R. Baker, D.L. Boone, et al. 2004. De-ubiquitination and ubiquitin ligase domains of A20 downregulate NF-kappaB signalling. Nature. 430:694–699. doi:10.1038/nature02794

JEM VOL. 207, July 5, 2010 1523